Opto-Electronic Advances

Supplementary information

August 2024, Vol. 7, No. 8

DOI: 10.29026/oea.2024.240076

Spin-controlled generation of a complete polarization set with randomly-interleaved plasmonic metasurfaces

Sören im Sande, Yadong Deng, Sergey I. Bozhevolnyi and Fei Ding*

Centre for Nano Optics, University of Southern Denmark, Odense 5230, Denmark.

*Correspondence: F Ding, E-mail: feid@mci.sdu.dk

Supplementary information for this paper is available at https://doi.org/10.29026/oea.2024.240076

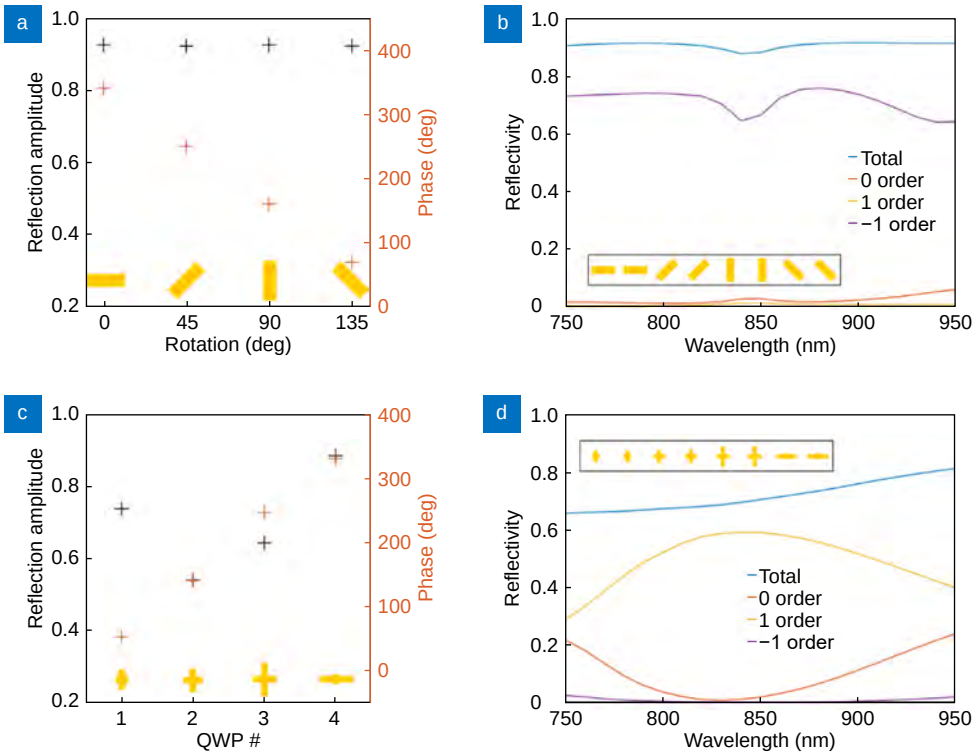

Fig. S1 | Performance of the meta-atoms under LCP incidence. (**a**) Simulated reflection amplitude and phase of the four HWP meta-atoms with different orientations at the design wavelength of 850 nm. (**b**) Simulated diffraction efficiencies of the HWP supercell, shown in the inset, as a function of wavelength. (**c**) Simulated reflection amplitude and phase of the four QWP meta-atoms at the design wavelength of 850 nm. (**d**) Simulated diffraction efficiencies of the QWP supercell, shown in the inset, as a function of wavelength. The dimensions of all selected meta-atoms are shown in Table S1.

Table S1 | Dimensions of the metaatoms.

Element	L_x (nm)	L_y (nm)
HWP	314	112
QWP #1	92	146
QWP #2	148	168
QWP #3	169	254
QWP #4	262	82

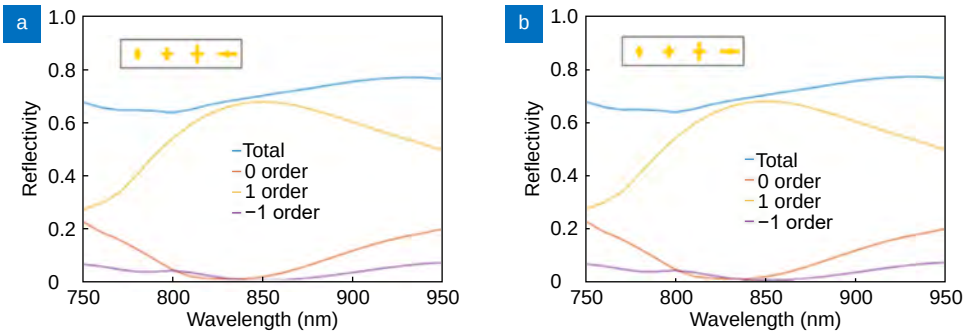

Fig. S2 | Simulated diffraction efficiencies of the QWP supercell consisting of 4 elements at the design wavelength of 850 nm under (**a**) RCP and (**b**) LCP incidence.

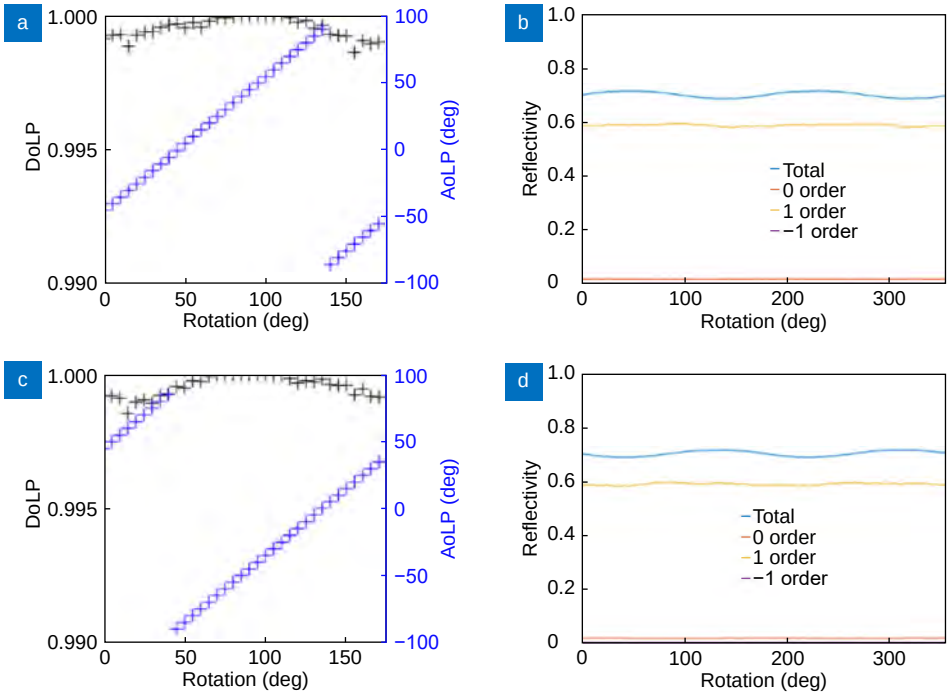

Fig. S3 | Performance of the QWP meta-atoms under different orientations at the design wavelength of 850 nm. (**a**) Simulated DoLP and AoLP of the beam within +1 diffraction order under LCP incidence. (**b**) Simulated diffraction efficiencies under LCP incidence. (**c**) Simulated DoLP and AoLP of the beam within +1 diffraction order under RCP incidence. (**d**) Simulated diffraction efficiencies under RCP incidence. The QWP supercell consists of 8 elements with varied orientations.

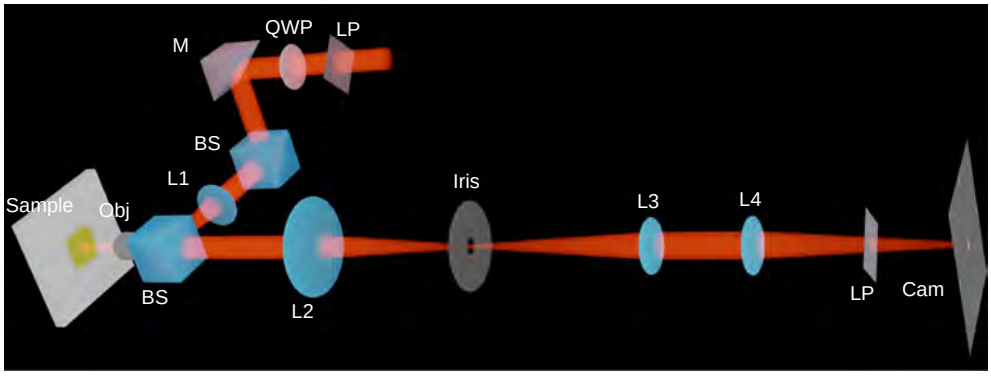

Fig. S4 | Schematic of the optical setup for the measurement. LP: linear polarizer; QWP: quarter wave plate; M: mirror; BS: beam splitter; L1-L4: lenses; Obj: objective.

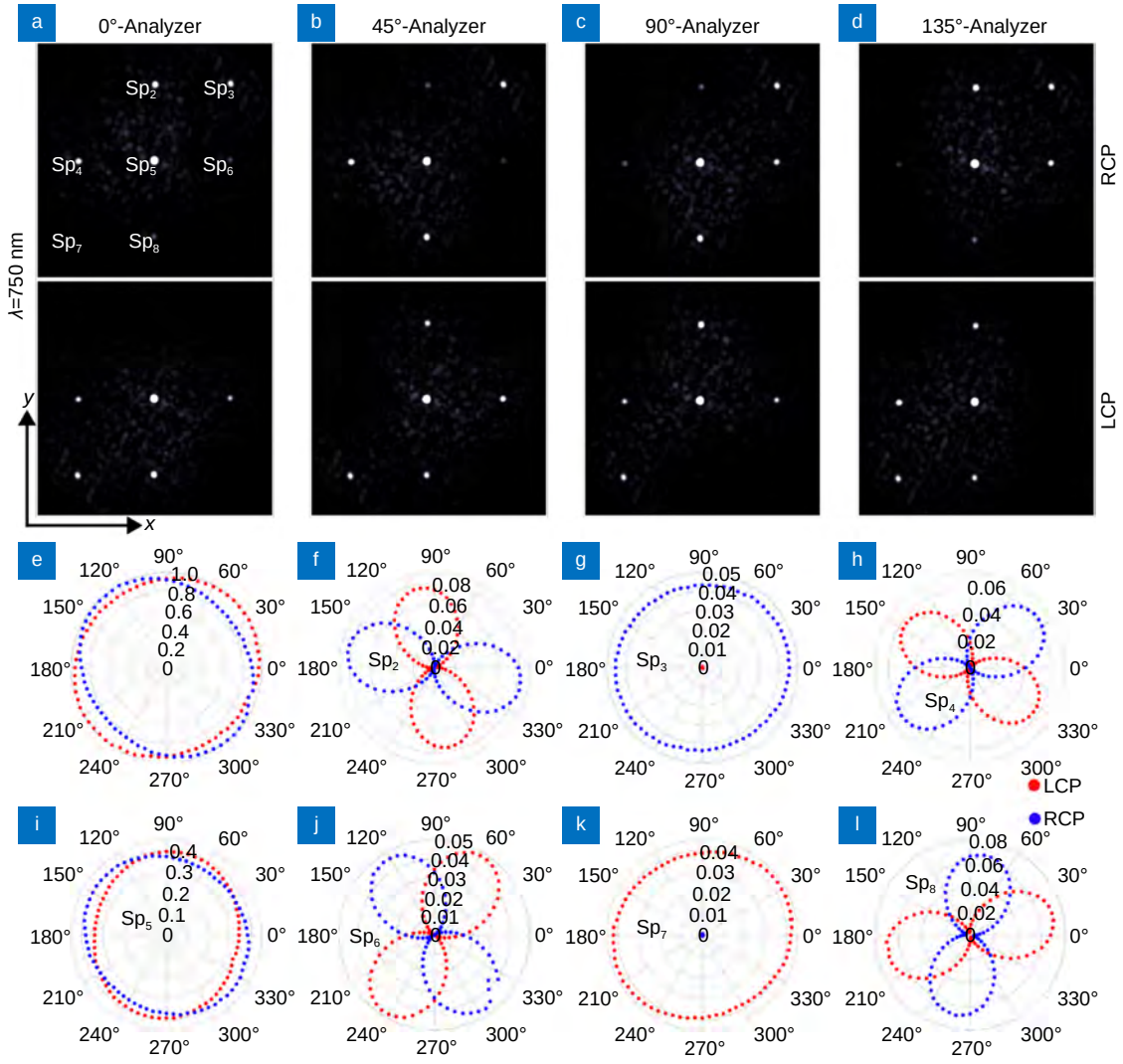

Fig. S5 | Experimental demonstration of spin-controlled full-polarization generation at the wavelength of 750 nm. (**a**–**d**) Polarization-resolved intensity profiles. The feature spots are marked as Sp_2-Sp_8. (**e**) Polar plots of the RCP (blue) and LCP (red) incident beams. (**f**, **h**, **j**, and **l**) Polar plots of the diffracted LP beams (Sp_2, Sp_4, Sp_6, and Sp_8) from the QWP meta-pixels with cross arms oriented at −45° (f), 0° (h), 90° (j), and 45° (l), respectively. The AoLPs are rotated by 90° once the incident light is switched from RCP to LCP. (**g**, **k**) Polar plots of the diffracted CP beams (Sp_3 and Sp_7) from the HWP meta-pixels. Only the cross-polarized CP beam is visible, with its handedness altered by the spin of incident light. (**i**) Polar plot of reflected CP beams (S_5) with co-polarization states from the mirror meta-pixels.

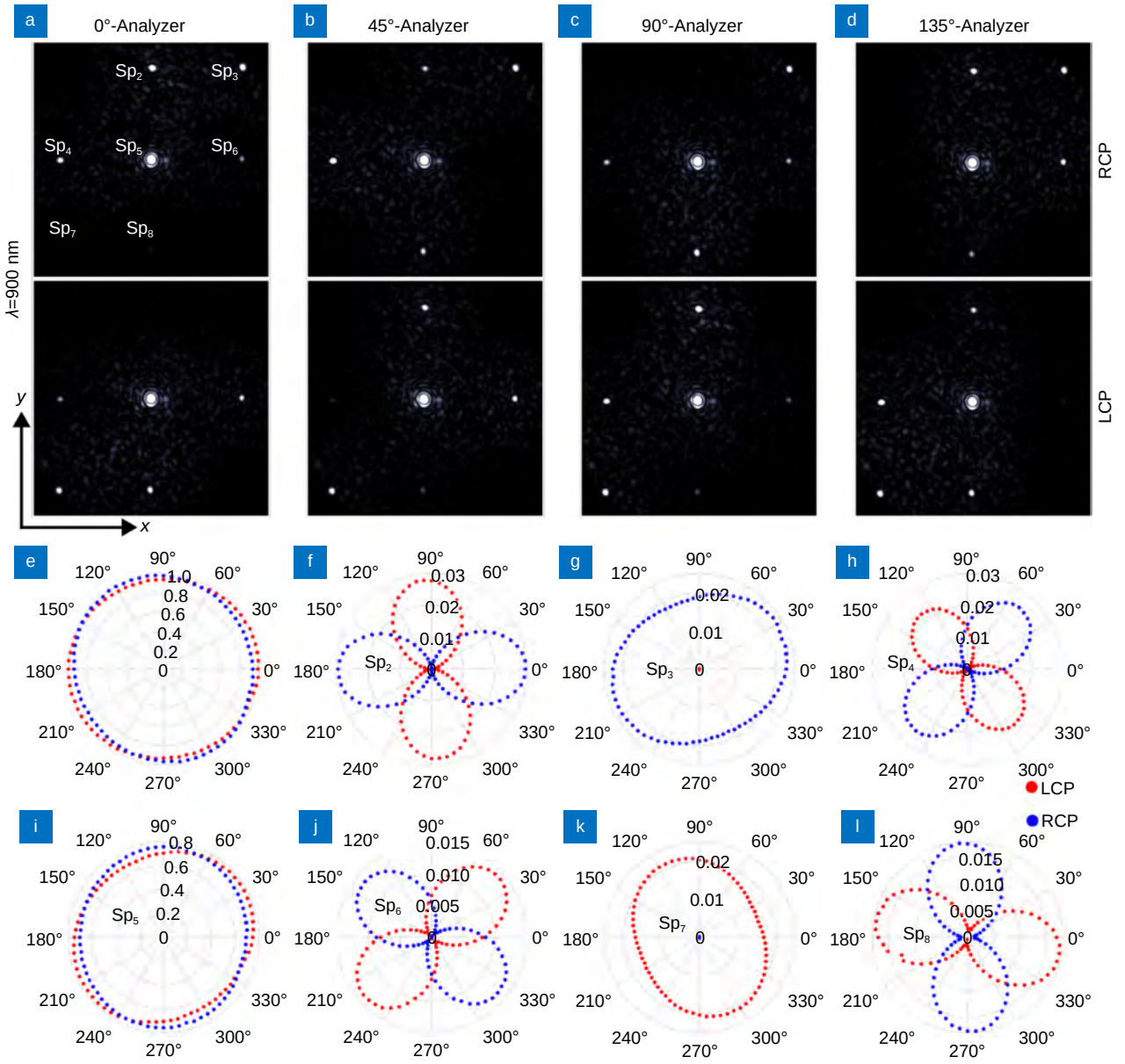

Fig. S6 | Experimental demonstration of spin-controlled full-polarization generation at the wavelength of 900 nm. (**a**–**d**) Polarization-resolved intensity profiles. The feature spots are marked as Sp_2-Sp_8. (**e**) Polar plots of the RCP (blue) and LCP (red) incident beams. (**f**, **h**, **j**, and **l**) Polar plots of the diffracted LP beams (Sp_2, Sp_4, Sp_6, and Sp_8) from the QWP meta-pixels with cross arms oriented at −45° (f), 0° (h), 90° (j), and 45° (l), respectively. The AoLPs are rotated by 90° once the incident light is switched from RCP to LCP. (**g**, **k**) Polar plots of the diffracted CP beams (Sp_3 and Sp_7) from the HWP meta-pixels. Only the cross-polarized CP beam is visible, with its handedness altered by the spin of incident light. (**i**) Polar plot of reflected CP beams (S_5) with co-polarization states from the mirror meta-pixels.

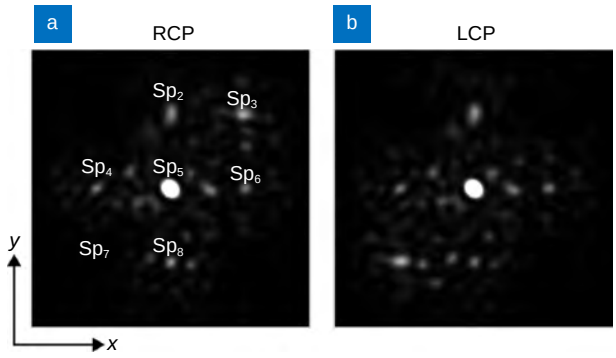

Fig. S7 | Simulated performance of a randomly interleaved metasurface with a reduced area of 19 μm × 19 μm (6 × 6 meta-pixel array) for spin-controlled polarization set generation at the design wavelength of 850 nm under (**a**) RCP and (b) LCP incidence. The efficiencies and retrieved Stokes parameters of spots Sp_2 to Sp_8 are listed in Tables S2 and S3.

Table S2 | Simulated efficiencies under RCP and LCP incidence.

	Sp_2	**Sp_3**	**Sp_4**	**Sp_5**	**Sp_6**	**Sp_7**	**Sp_8**	**Noise**
RCP	0.06	0.126	0.06	0.4	0.11	0.002	0.08	0.15
LCP	0.06	0.003	0.05	0.4	0.12	0.144	0.08	0.15

Table S3 | Simulated Stokes parameters under RCP and LCP incidence.

	Sp_2	**Sp_3**	**Sp_4**	**Sp_5**	**Sp_6**	**Sp_7**	**Sp_8**
RCP	$S_1 = -0.98$	$S_3 = -0.98$	$S_2 = 0.99$	$S_3 = 0.99$	$S_2 = 0.97$	NA	$S_1 = -0.98$
LCP	$S_1 = 0.96$	NA	$S_2 = -0.99$	$S_3 = -0.99$	$S_2 = -0.97$	$S_3 = 0.98$	$S_1 = 0.99$

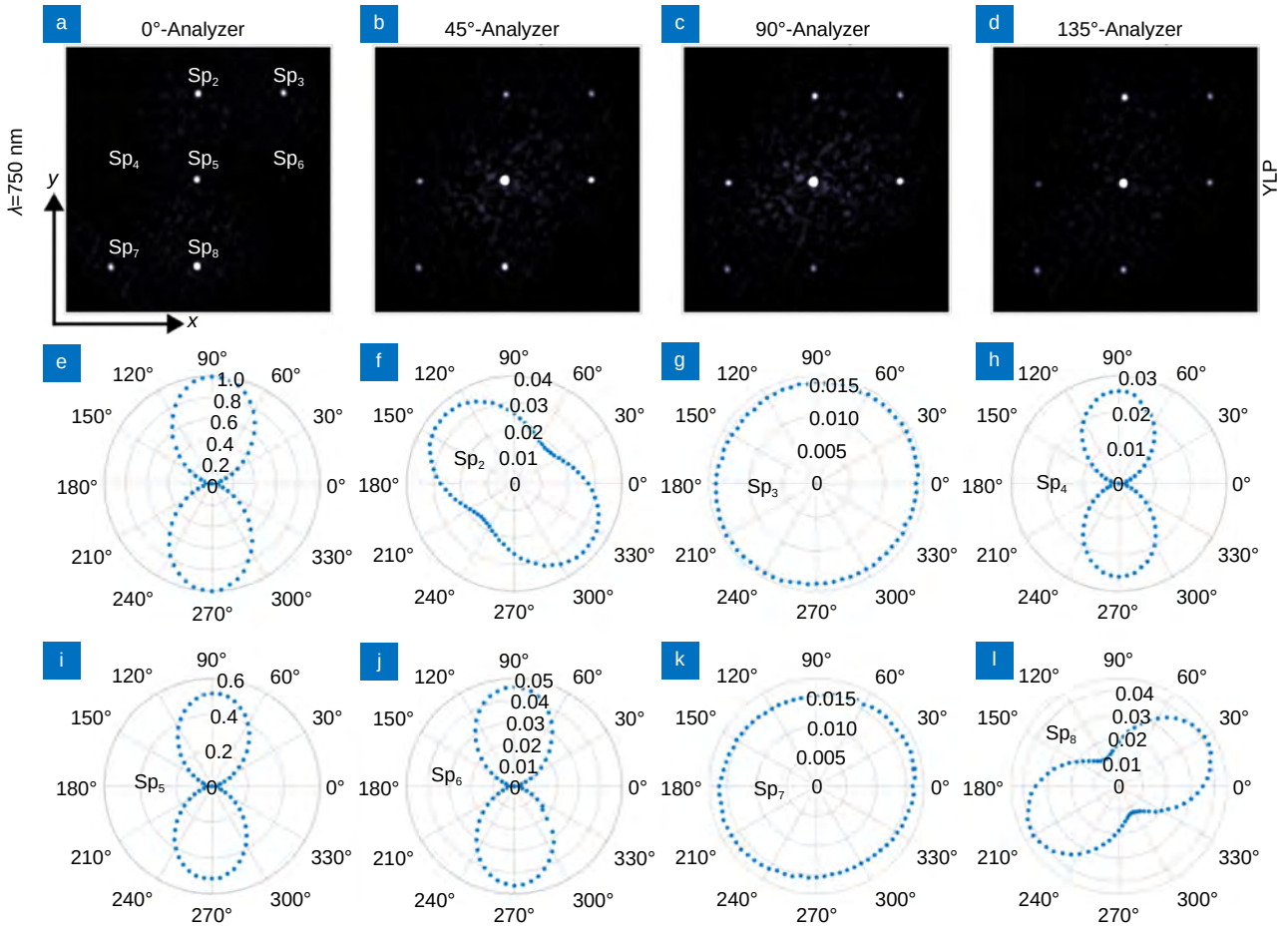

Fig. S8 | Operation performance of the metasurface for *y*-polarized incident light at the wavelength of 750 nm. (**a**–**d**) Polarization-resolved intensity profiles. The feature spots are marked as Sp_2-Sp_8. (**e**) Polar plot of the *y*-polarized incident beam. (**f** and **l**) Polar plots of the diffracted elliptically polarized beams (Sp_2 and Sp_8) from the QWP meta-pixels with cross arms oriented at −45° (f) and 45° (l), respectively. (**g**, **k**) polar plots of the diffracted CP beams (Sp_3 and Sp_7) from the HWP meta-pixels. Both LCP and RCP beams are visible. (**h**, **j**) polar plots of the diffracted *y*-polarized beams (Sp_4 and Sp_6) from the QWP meta-pixels with cross arms oriented at 0° (h) and 90° (j), respectively. (**i**) polar plot of the reflected *y*-polarized beam (Sp_5) from the mirror meta-pixels.

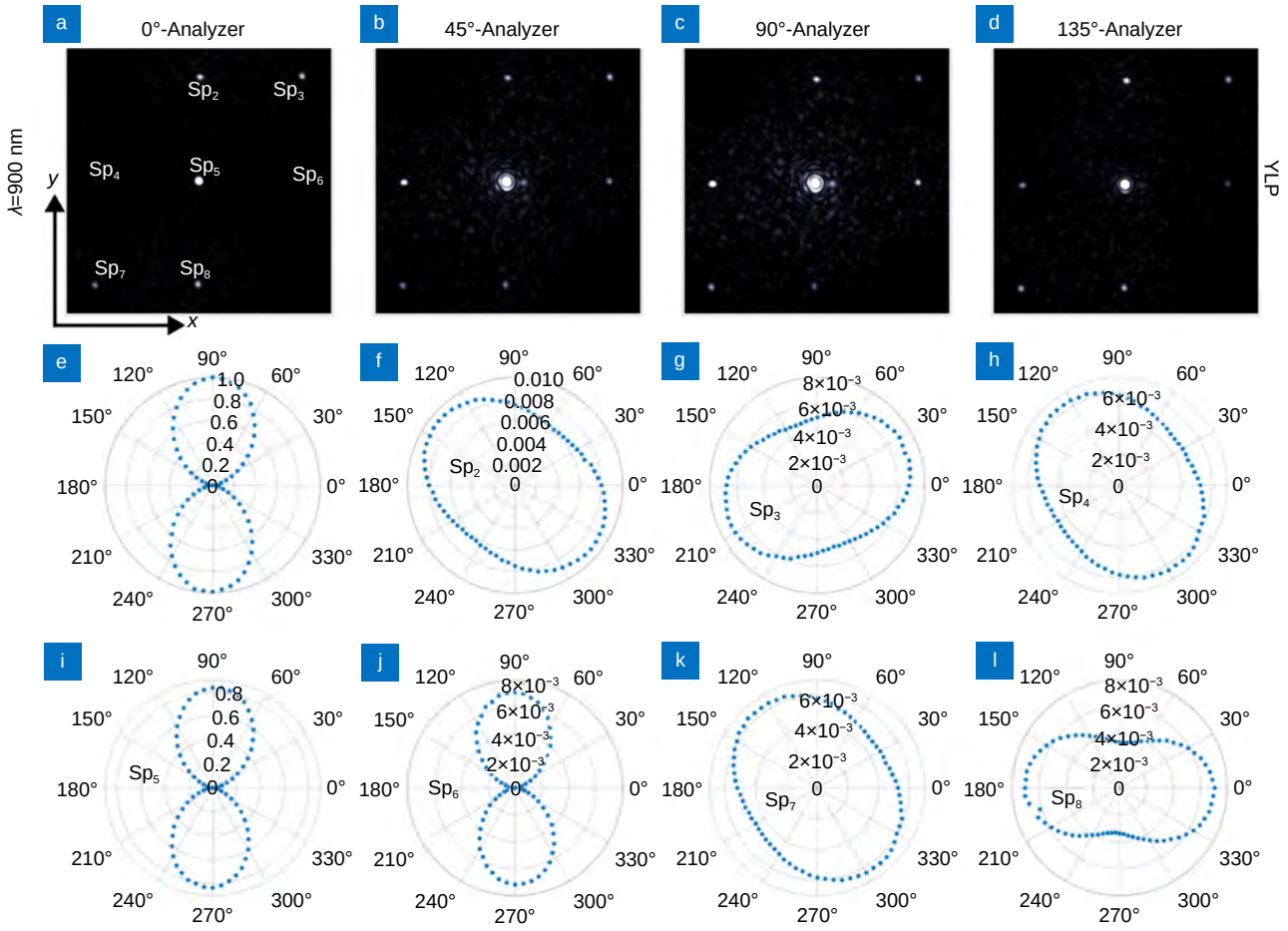

Fig. S9 | Operation performance of the metasurface for *y*-polarized incident light at the wavelength of 900 nm. (**a**–**d**) Polarization-resolved intensity profiles. The feature spots are marked as Sp_2-Sp_8. (**e**) Polar plot of the *y*-polarized incident beam. (**f**, **l**) polar plots of the diffracted elliptically polarized beams (S_2 and S_8) from the QWP meta-pixels with cross arms oriented at −45° (f) and 45° (l), respectively. (**g**, **k**) Polar plots of the diffracted CP beams (Sp_3 and Sp_7) from the HWP meta-pixels. Both LCP and RCP beams are visible. (**h**, **j**) polar plots of the diffracted *y*-polarized beams (Sp_4 and Sp_6) from the QWP meta-pixels with cross arms oriented at 0° (h) and 90° (j), respectively. (**i**) Polar plot of the reflected *y*-polarized beam (Sp_5) from the mirror meta-pixels.